Supplementary Information to "Correlations of neuronal and microvascular densities in cortex revealed by direct counting and colocalization of nuclei and microvessels".

Supplemental Figure 1. Deep antibody labeling and simultaneous imaging of labeled vasculature, nuclei and neuronal nuclei. A brain from a NIH Swiss mouse was perfused then simultaneously stained with DAPI to label all cellular nuclei and α-NeuN directly conjugated to Alexa-594 to specifically label neuronal nuclei. The tissue was treated with 2.0 % Triton X-100 and cleared by gradual immersion to 60% sucrose. **(a)** Overlay of the maximal X-Z projections of the fluorescein (vessel) and DAPI (cell nuclei) channels. **(b)** Overlay of the maximal X-Z projections of the fluorescein (vessel) and Alexa594 (neuronal nuclei) channels. **(c)** Overlay of the maximal X-Z projections of all three channels taken from the 700 µm deep region highlighted by the red rectangle in panels (a) and (b).

Supplemental Figure 2. Coronal sections of mouse brain depict the regions of cortex used for volumetric data analysis. Coronal sections, 40 µm in thickness, were taken from a C57BL/6 mouse in which retinal projections were labeled using cholera toxin B. Sections stained with a Nissl-like Giemsa stain prior to being scanned with a ScanScope® XT (Aperio Technologies, Vista, CA) line scanning system. **(a - c)** Coronal sections taken at the Bregma + 1 mm (a), bregma - 1 mm (b) and bregma - 2 mm (c) positions used for volumetric data analysis. **(d - f)** Magnified images from the regions that are highlighted in red in panels (a) to (c). The images span the region that lie between 0.8 and 1.4 mm from the midline in each section, and correspond to the regions from which volumetric data was collected. **(g)** Magnified image of the whisker barrel field region highlighted in blue in panel (b). White arrows point to regions of prominent granule cells. Yellow arrows point to the septae between whisker barrels. **(h)** High magnification view of the area highlighted in white in panel (e). The left half of the image contains a distinct granular layer 4, whereas the right half of the image is agranular. The gray band approximates the zone of transition from granular to agranular cortex.

Supplemental Figure 3. Comparison of vessel diameters from histological and *in vivo* preparations. (a) Two photon laser scanning microscopy image stack from an awake mouse through a thinned-skull preparation. An average projection was taken across 30 µm in the axial direction for visualization. The four adjoining line plots show the relative intensity along the perpendicular to the four vessels highlighted with colored bars in the image. The correspondingly colored bar in the plot shows the diameter of the vessel measured at the appropriate fractional threshold, according to the same simulation-based look-up table used in the histological analysis algorithms. (**b1 - b9**) Comparative histograms of the

vessel diameters from an awake animal (thin black bars) and nine representative histological specimen from different animals (thick gray bars). The *in vivo* histogram is repeated and overlaid on the nine histological histograms for ease of comparison. In both cases, the analyzed region spanned depths of 25 to 100 µm below the pial surface. (**c**) A single histogram containing the vessel diameters of 45 histological volumes (thick gray bars, compilation of 15 animals, 3 rostral-caudal positions each). The *in vivo* histogram is overlaid (thin black bars) for ease of comparison.

Supplemental Figure 4. **Subjective thresholding can yield large variations in fractional volume of vasculature.** This reanalysis highlights potential errors in past estimations of fractional vascular volume. **(a1 - a4)** A single two photon laser scanning microscopy image frame of labeled vasculature displayed at four different gamma settings: (a1) $\gamma = 1$, (a2) $\gamma = 0.75$, (a3) $\gamma = 0.50$, and (a4) $\gamma = 0.25$. **(b1 - b4)** Magnified view of the highlighted region in panels (a1) to (a4). The apparent size of the structures depends strongly on the display setting, as illustrated by the yellow voxel outlines. **(c1 - c4)** The same field of view as in panels (a1) to (a4) displayed on a linear color map ($\gamma = 1$) across the relative intensity values of (c1) 0 to 100 %, (c2) 0 to 50 %, (c3) 0 to 25 %, and (c4) 0 to 0 %. **(d1 - d4)** Magnified view of the highlighted region in panels (c1) to (c4). As above, the apparent size of structures depends heavily on the display setting. (**e**) The intensity profile across the horizontal voxel row highlighted by yellow boxes in panels (b) and (d). **(f)** The profile in panel (e) after thresholding at different fractions of the maximum intensity. Note the widely varying values for both the vessel diameter and the fractional volume of the vasculature in the full image field.

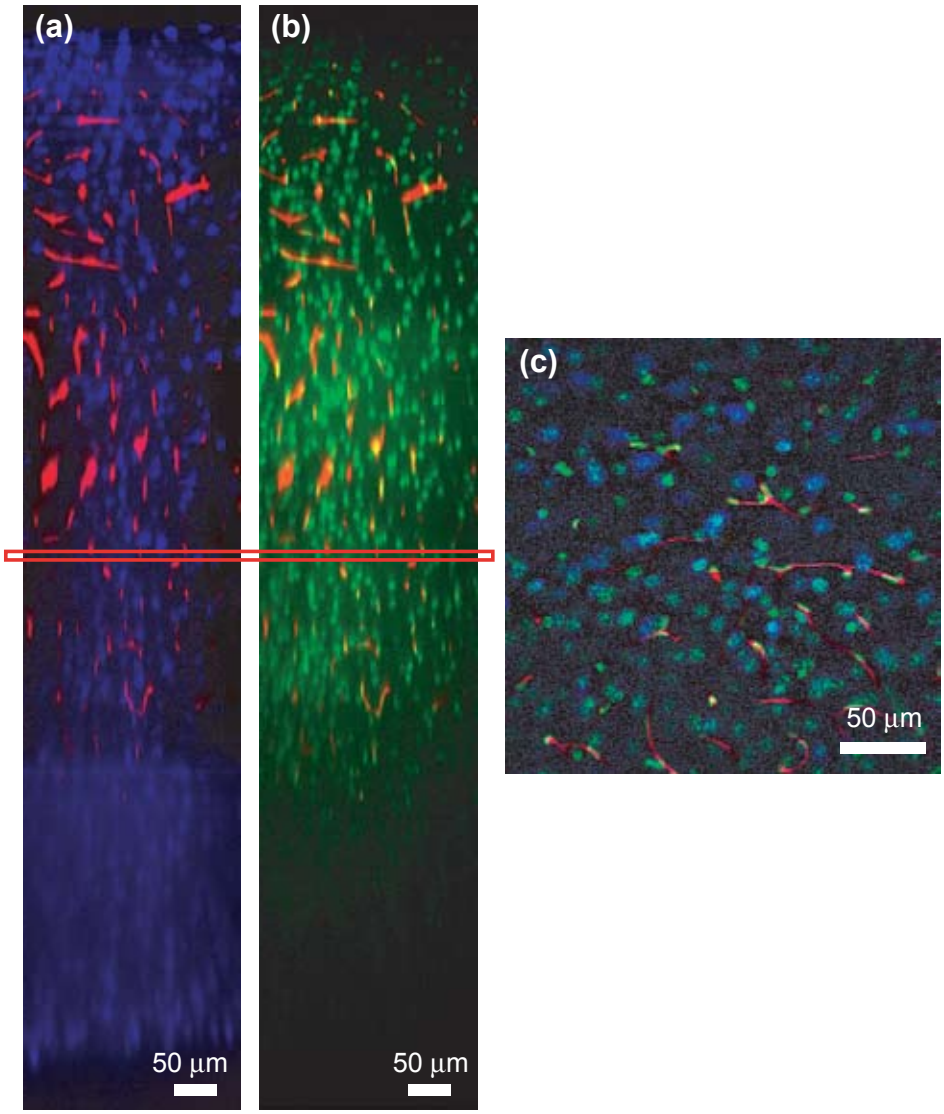

Supplemental Figure 1. Tsai et al. submission

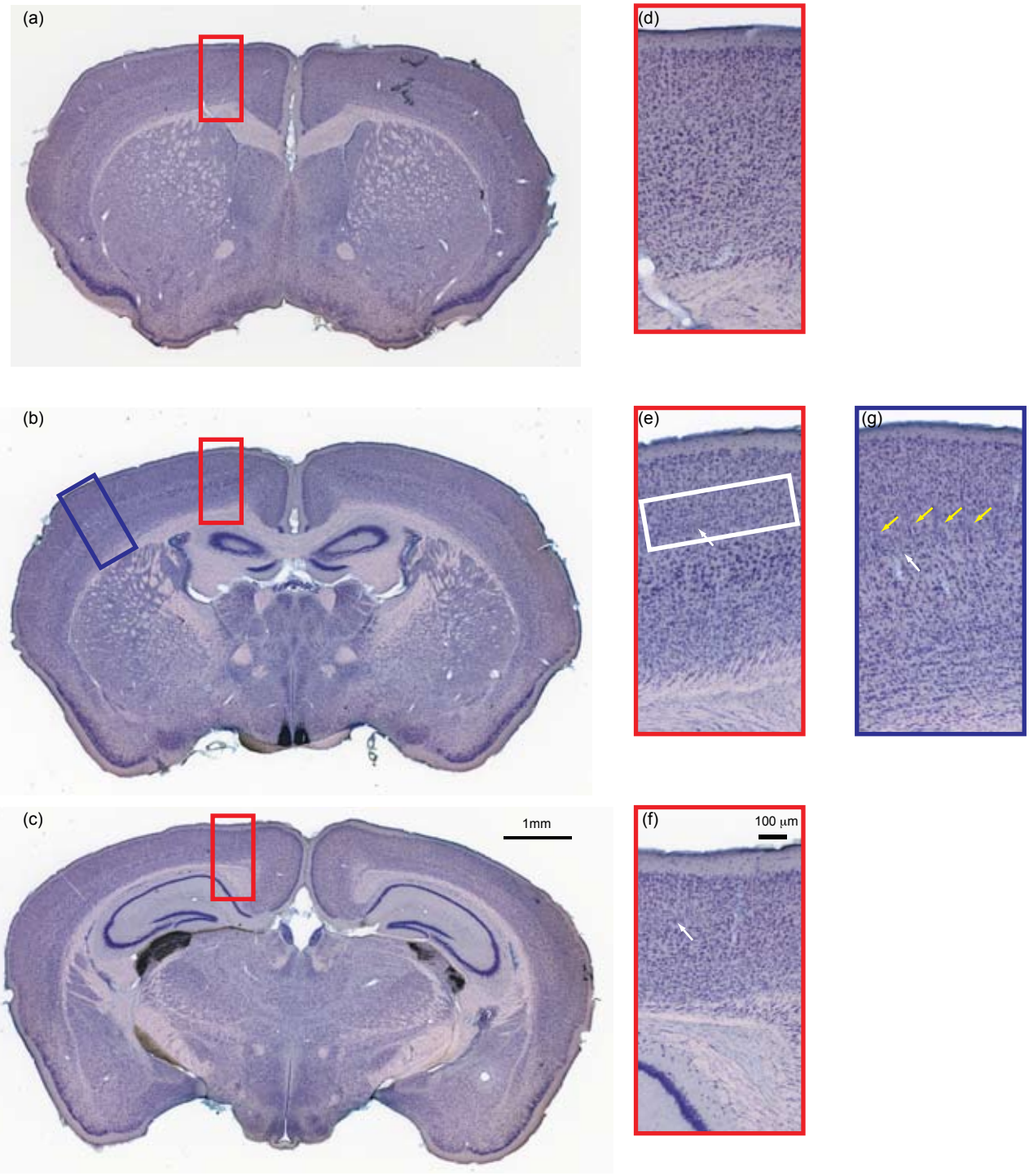

Supplemental Figure 2, Tsai et al.

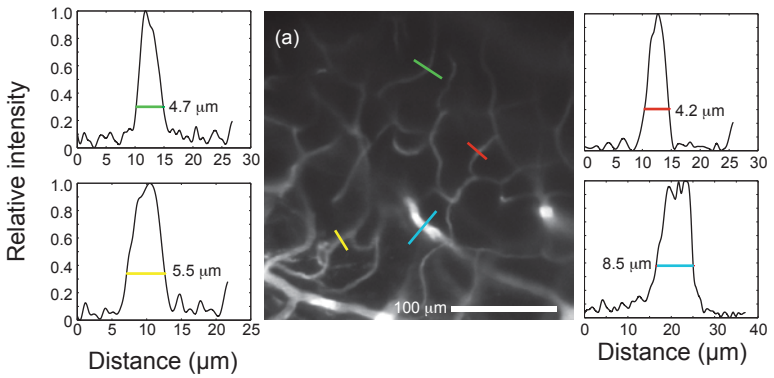

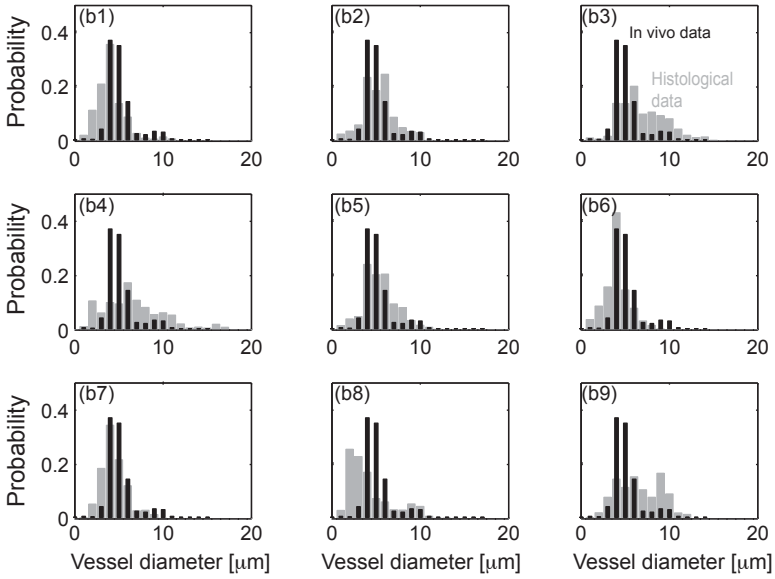

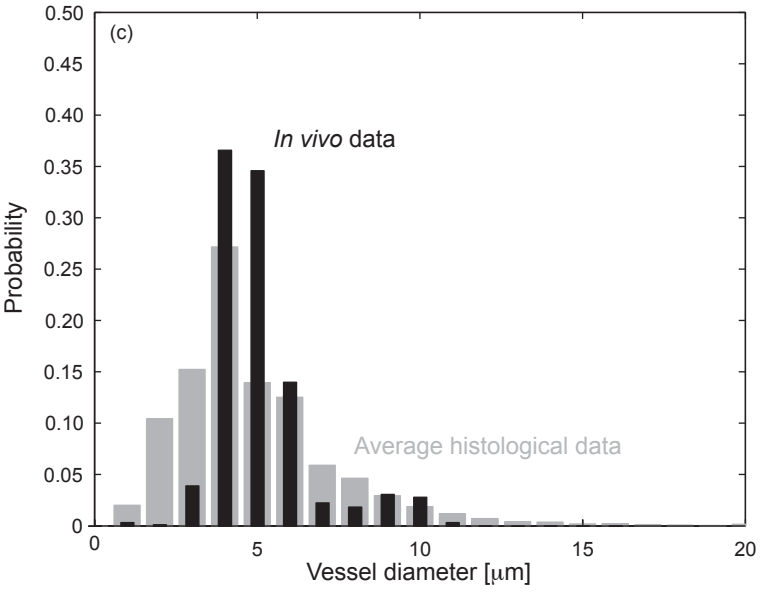

Supplemental Figure 3, Tsai et al.

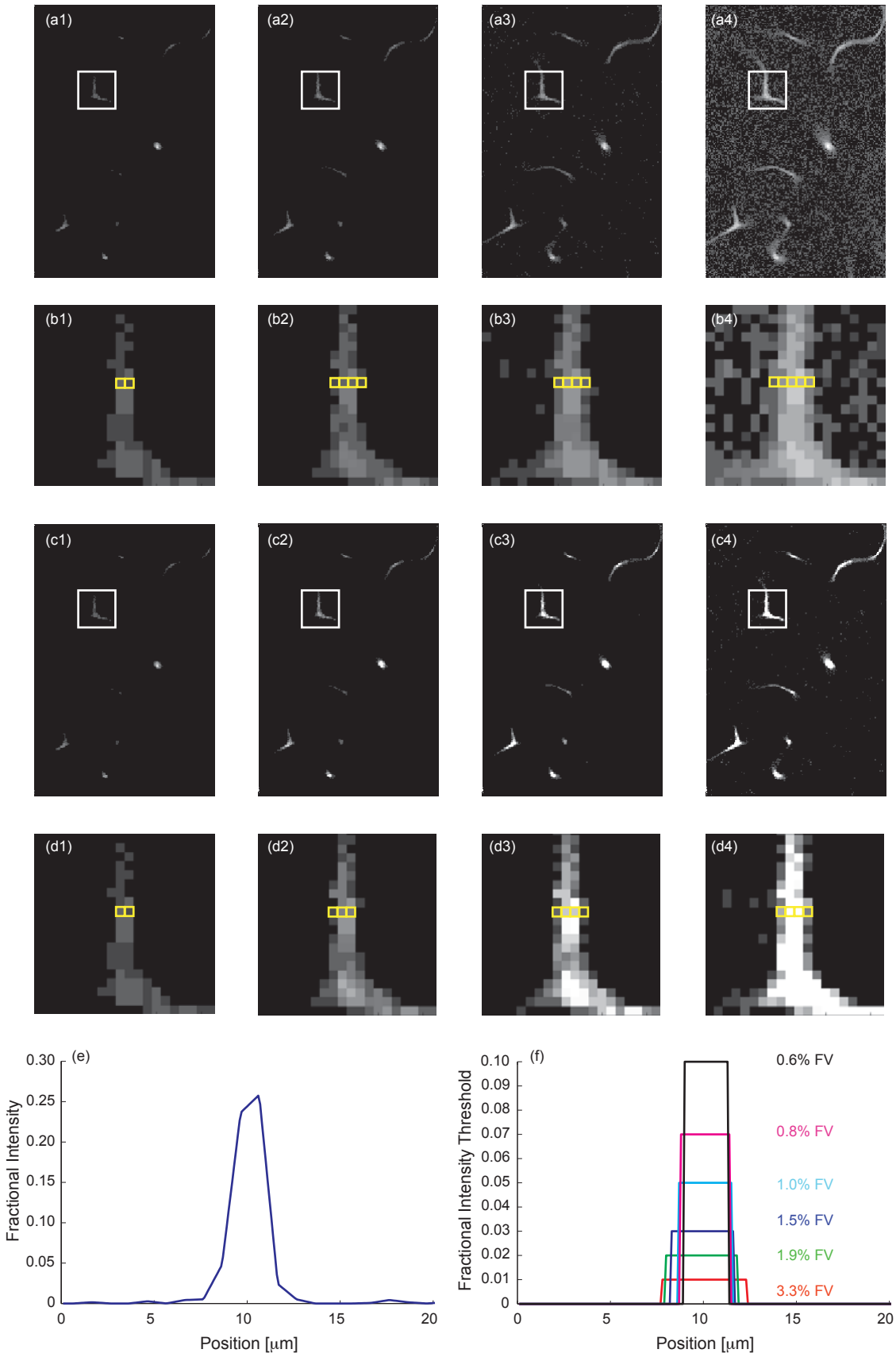

Supplemental Figure 4, Tsai et al.

Supplementary Table 1. Sensitivity values for nuclei counts, n

Procedure	VIDA code parameter (p)	Figure	Base p_0	$\frac{\partial(n/n_0)}{\partial(p/p_0)}$	$\frac{1}{2}\frac{\partial^2(n/n_0)}{\partial(p/p_0)^2}$
Cell segmentation	cellMatchFilterModelVariance, $2\sigma^2_{\text{cell-local}}$	6a,b	8	**-0.13**	**0.16**
	cellMatchFilterBackgroundVariance, $2\sigma^2_{\text{cell-bkg}}$	6a,b	40	**-0.10**	**0.17**
	cellMatchFilterNumSigma, z	6b,c	5	-0.10	-0.05
	cellMatchFilterMinimumVolume	6b,c	100	-0.06	0.02
	cellMatchFilterMaxVolumePercent	6b,c	0.1	<0.01	--
Cell centroid isolation	cellCentriodBlockSizeY	6c,c	40	0.00	0.02
	cellCentroidBufferZoneY	6c,c	10	-0.01	-0.02
	cellCentroidMergeDist, $D_{\text{cell\_min}}$	6d,e	5	**-0.10**	0.02

Supplementary Table 2. Sensitivity values for the number, n, of nuclei classified as neurons

Procedure	VIDA code parameter (p)	Figure	Base p_0	$\frac{\partial(n/n_0)}{\partial(p/p_0)}$	$\frac{1}{2}\frac{\partial^2(n/n_0)}{\partial(p/p_0)^2}$
Neun quantification	vascMaskFilterSize	9a	3	0.01	-0.01
	minCellAnalysisVolume	9a	9	<0.01	--
	minBkgAnalysisVol	9a	9	<0.01	--
	mainCell	9a	2	0.05	-0.05
	bkgShell	9a	7	-0.03	-0.01
	otherCell	9a	4	-0.02	0.02
Neuronal classification	ratioNeighborhoodXY	9c	50	-0.01	0.01
	ratioNeighborhoodZ	9c	10	<0.01	--
	minRatioThresh	9c	0.05	<0.01	--
	maxRatioThresh	9c	0.15	<0.01	--
	convergenceFraction	9c	0.01	<0.01	--

Supplementary Table 3. Sensitivity analysis of the backbone contribution to vascular volume, v.

Procedure	VIDA code parameter (p)	Figure	Base p_0	$\frac{\partial(v/v_0)}{\partial(p/p_0)}$	$\frac{1}{2}\frac{\partial^2(v/v_0)}{\partial(p/p_0)^2}$
Vascular rod filter	rodFilterHalfSize	7a-c	5	0.01	0.05
	numPointsRodFilter	7a-c	4	<0.01	--
	numTrianglesRodFilter	7a-c	2	<0.01	--
Vessel segmentation raw	enhMaskPrelimThresholdFraction	7c-i	0.05	<0.01	--
	numBkgStdForMinThresh	7a-i	4.4	<0.01	--
	fractionOfHighIntensityForMaxThresh	7a-i	0.15	<0.01	--
	filtMultiplierForVarThresh	7a-i	1.5	<0.01	--
	minVolForSmallVolRemoval	7a-i	27	<0.01	--
	numCleanupCycles	7a-i	3	<0.01	--
	gaussianRadiusForFilter	7a-i	11	-0.01	0.01
Vessel segmentation enhanced	enhMaskPrelimThresholdFraction	7c,d	0.05	<0.01	--
	numBkgStdForMinThresh	7d-i	4.4	<0.01	--
	fractionOfHighIntensityForMaxThresh	7c,d	0.1	<0.01	0.01
	numCleanupCycles	7c,d	10	0.02	0.01
	filtMultiplierForVarThresh	7c,d	0.1	-0.01	<0.01
	minVolForSmallVolRemoval	7c,d	27	<0.01	--
	gaussianRadiusForFilter	7c,d	21	0.02	<0.01
Vessel centerlining	preCloseDiameter	7d-l	7	<0.01	--
	maxFlips	7e,f	15	<0.01	--
	hairTrimRadiusMultiplier	7f,g	1	<0.01	--
	hairTrimRadiusAdditive	7f,g	2	<0.01	--
	maxCenteringFieldFilterRange	7d-l	120	<0.01	--
	centeringIterMultiplier	7d-l	0.5	<0.01	--
	smallLoopCleanupSize	7g,h,m	5	-0.01	0.01
	minVolForConnectedCenterLine	7g,h	5	-0.01	0.01

Supplementary Table 4. Sensitivity analysis of the radial contribution to vasculare volume, v

Procedure	VIDA code parameter (p)	Figure	Base p_0	$\frac{\partial(v/v_0)}{\partial(p/p_0)}$	$\frac{1}{2}\frac{\partial^2(v/v_0)}{\partial(p/p_0)^2}$
Vessel reconstruction	neighborhoodSizeFactor	8a,8b - 8d	6	<0.01	--
	minNeighborhoodSize	8a - 8d	6	<0.01	--
	localRadiiMultiplerForSaturation	8b,8c - 8e	0.5	-0.01	0.00
	brightValueFraction	8c - 8e	0.1	**0.14**	-0.05
	firstRoundThresholdFraction	8e - 8f	0.389	**0.10**	-0.03
	maxLocalRadius	8c - 8e	10	<0.01	--
	maxFractionOfSubFramePixels	8e - 8f	0.25	<0.01	--
	maxPixelAreaForNoiseBlock	8e - 8f	27	<0.01	--
	closeDiameter	8f - 8g	3	**0.10**	0.00
	interpolateFactor	8f - 8g	1	-0.02	0.01
	bwDistSearchWindowSize	8g - 8h, 8i	3	**0.18**	-0.06
	minVesselRadiusSupport	8g - 8h, 8i	0.5	<0.01	--
	zSearchSize	8g - 8h, 8i	3	0.02	-0.03

Supplementary Table 5. Sensitivity analysis for the vascular volume classified as microvasculature

Procedure	VIDA code parameter (p)	Figure	Base p_0	$\frac{\partial(l/l_0)}{\partial(p/p_0)}$	$\frac{1}{2}\frac{\partial^2(l/l_0)}{\partial(p/p_0)^2}$
Microvessel isolation	blockSize		300	<0.01	--
	blockOverlapSize		40	<0.01	--
	deltaR		3	0.02	0.01